Comparison of Simple Self-Oscillating PWM Modulators

Dahl, Nicolai J.; Iversen, Niels Elkjær; Knott, Arnold; Andersen, Michael A. E.

Published in:
Proceedings of the 140th Audio Engineering Convention Convention.

Publication date:
2016

Document Version
Peer reviewed version

Audio Engineering Society

Convention Paper

Presented at the 140th Convention
2016 June 4–7, Paris, France

Comparison of Simple Self-Oscillating PWM Modulators

Nicolai J. Dahl, Niels E. Iversen, Arnold Knott, and Michael A.E. Andersen

Technical University of Denmark

Correspondence should be addressed to Niels Iversen (neiv@elektro.dtu.dk)

ABSTRACT

Switch-mode power amplifiers has become the conventional choice for audio applications due to their superior efficiency and excellent audio performance. These amplifiers rely on high frequency modulation of the audio input. Conventional modulators use a fixed high frequency for modulation. Self-oscillating modulators do not have a fixed modulation frequency and can provide good audio performance with very simple circuitry. This paper proposes a new type of self-oscillating modulator. The proposed modulator is compared to an already existing modulator of similar type and their performances are compared both theoretically and experimentally. The result show that the proposed modulator provides a higher degree of linearity resulting in around 2 % lower Total Harmonic Distortion (THD).

1 Introduction

Switch-mode power amplifiers have become the conventional choice for audio applications during the last decade. This is due to the superior efficiency these amplifiers offer, compared with traditional linear amplifiers. For audio applications efficiencies in the vicinity of 90% have been achieved as shown in [1] and [2]. Also in terms of linearity switch-mode power amplifiers have shown great performance with Total Harmonic Distortion as low as 0.001%, [3] and [4]. The switch-mode power amplifier works by modulating the input audio into a high frequency pulse train which drives a power stage, typically equipped with MOSFETs. The linearity of the modulation is important for the overall distortion of the amplifier. Conventionally the modulator modulates the audio input at a fixed high frequency. However this can introduce Electro Magnetic Interference (EMI) issues. Self-oscillating oscillators does not have a fixed modulation frequency and therefore this type of modulator is preferable for EMI reasons [5]. Moreover the circuit complexity is reduced when using this type of modulators.

This paper will describe the fundamental principles of Pulse Width Modulation (PWM) and examine how this can be generated in self-oscillating modulators. A new type of self-oscillating modulator will be presented and compared to an already existing self-oscillating modulator topology. A thorough analysis of both modulators will be presented in order to evaluate their linearity. Finally measured results obtained from implemented test boards will be presented to support the theoretical analysis.

2 Modulator

2.1 Principles

The function of a modulator in a switch mode audio amplifier is to convert a continuous audio signal to a pulse coded signal. Among the different types of

pulse coding the Pulse Width Modulation is the most commonly used for switch mode audio amplifiers [6]. PWM works by changing the percentage of time the output is high compared to the time the output is low. Depending on the current value of the audio signal, the aforementioned percentage will change. This property is called the duty cycle and with PWM it is possible to obtain a unique duty cycle for each unique value of the audio signal. The duty cycles spectrum can further be described with the modulation index which is a value that tells how much of the spectrum the modulation should span over.

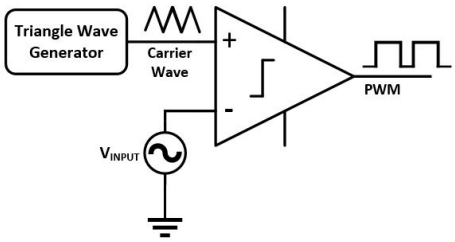

Fig. 1: Concept of a modulator

Figure 1 shows a simple hardware realization. By comparing the audio signal with a triangle signal, also called the carrier waveform, it is possible to create a PWM signal. However, to get a good representation of the audio signal the carrier waveform needs to run at a frequency that is much higher than the highest audible frequency. This is necessary to get a high resolution of the audio signal. The PWM signal is fed to the power stage of the amplifier which amplifies the signal. Finally a lowpass filter removes the high switching frequency thus restoring the original audio signal. The reason a triangle waveform is used as the carrier waveform is that the triangle provides a constant relationship between the audio signal and the corresponding duty cycle. In practice this means that the modulator will not induce any harmonic distortion to the audio signal as long as the amplitude of the audio signal does not exceed the amplitude of the carrier waveform. If the audio signals amplitude exceeds the amplitude of the carrier waveform clipping would happen.

While this method is able to create a great transparent modulation it has some drawbacks. The carrier waveform is run at a fixed frequency which will result in a build-up of spectral energy at the carrier frequency and its harmonics [5]. This can introduce unwanted EMI. Moreover the size of the circuitry is also large compared to other implementations of PWM modulators due to the need of an external triangle generator [12]. One way to address these problems is by using the self-oscillating modulator topology.

2.2 Self-Oscillating Modulators

Self-oscillating modulator are a branch of modulators where the carrier waveform generator circuitry has been merged with the comparator circuitry thus making it possible to reduce the amount of components needed, [7], [8], [9] and [10]. The carrier waveform generation is achieved by feeding back the output of the modulator, through some circuitry, back into the comparator making the modulator oscillate. This also makes the switch frequency dependant of the input signal, ultimately reducing EMI [5]. To ensure that the modulator has a controlled oscillation a 180^o phase lag is introduced. This is typically done either by a hysteresis window or a phase shift [11].

2.2.1 Astable Integrating Modulator

One of the simplest self-oscillating modulators is the Astable Integrating Modulator (AIM) as presented in [12] shown in fig. 2.

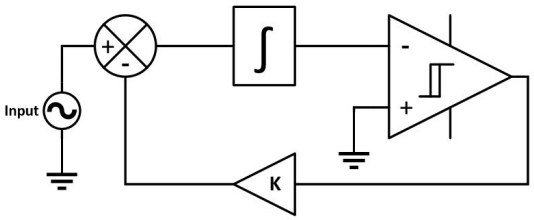

Fig. 2: Concept of the AIM

The AIM works by using its output with the audio input to calculate an error signal. The error signal is integrated to generate a triangle carrier waveform which is sent to a comparator with a hysteresis window. The hysteresis window is used to control the amplitude of the carrier waveform and by doing so it also controls the maximum carrier frequency also called the idle switch frequency. The idle frequency is controlled by

the gain factor K as well which controls the size of the error and therefore the slope of the integration. Figure 3 shows a possible way of implementing the AIM in hardware.

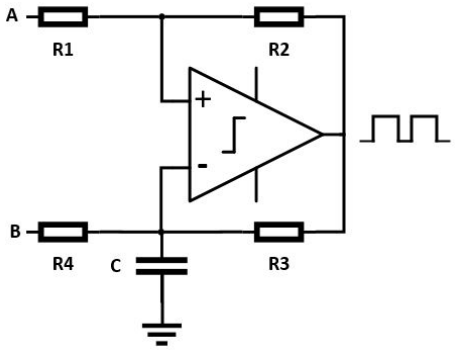

Fig. 3: Implementation of AIM and HOM

In fig. 3 the terminal A is connected to a reference voltage and terminal B is connected to the audio input. The reference voltage is used as the bias voltage for the entire modulator as well as the audio input. The hysteresis window is implemented using the resistors R_1 and R_2 while the error signal integration is realized using R_3, R_4 and C. The integration is implemented as a RC network which operation deviates from an ideal integration. While an ideal integrator generates a slope that is proportional to the error signal, the RC network generates an exponential response. This results in harmonic distortiondue to the fact that the RC network is not able to produce ideal triangles. Figure 4 shows this phenomenon.

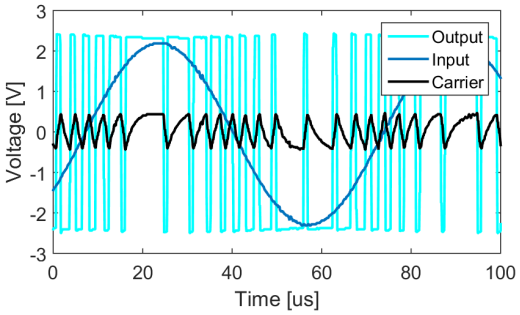

Fig. 4: Input, output and carrier for an AIM

The harmonic distortion can to a certain degree be reduced by reducing the size of the hysteresis window or reducing the modulation index. However, a reduction in the hysteresis window will result in smaller internal signals in the modulator thus making the modulator more sensitive to noise since the signal levels come closer to the noise floor. A reduction in the modulation index will result in a lower efficiency of the amplifier. This renders both solutions undesirable.

2.2.2 Hysteresis Offset Modulator

To address this problem of the AIM this paper proposes an alternative self-oscillating modulator consisting of the same circuitry as the AIM in fig 3. The main difference, between the AIM and the proposed modulator, is that the voltage reference and the audio input is swapped so that the audio signal is connected to terminal A and the voltage reference to terminal B. This makes the input signal offset the hysteresis window and hence it is named 'Hysteresis Offsetting Modulator' shorted HOM. This simple change completely changes the behaviour of the system which can be seen on fig. 5.

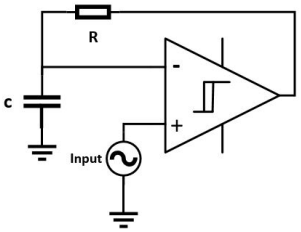

Fig. 5: Concept of the HOM

Unlike the AIM, where the RC network is a drawback for the performance due to the harmonic distortion the HOM actively exploits the properties of the RC network to make the modulation. By using the audio input to change the reference voltage of the comparator, the hysteresis window is constantly being offset. This results in the RC network constantly operating in different zones thus changing the slope more or less as seen on fig. 6.

3 Deriving of Models

To determine which of these two modulators introduces most harmonic distortion, mathematical models need to

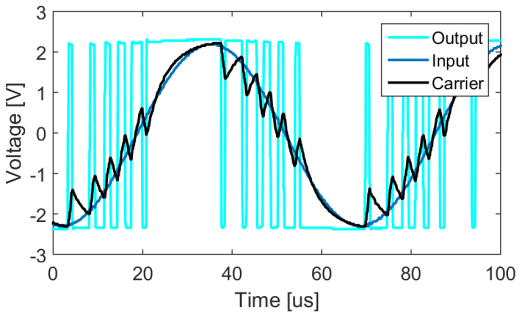

Fig. 6: Input, output and carrier of the HOM

be constructed. A similar approach has been presented in previous work for the AIM modulator [13]. The models will be constructed such that the performance of the modulator can be described by:

- The size of the hysteresis window
- The peak-peak voltage of the audio input
- The reference voltage
- The supply voltage

Since the two modulators share the same circuitry, many parts of the model will be identical. Both modulators generate a PWM output and therefore need an equation for describing the time the output is high as well as an equation to describe the time the output is low. The two states of the output are defined as:

$$v_{out}(t) = \begin{cases} v_H & \forall v_C(t) < v_{hys}(t) \\ v_L & \forall v_C(t) > v_{hys}(t) \end{cases} \quad (1)$$

Where v_H and v_L is the high and low voltage given on the output of the modulator. v_C and v_{hys} is the voltage of the carrier waveform and hysteresis window respectively for any given time.

The hysteresis window works identically for the two modulators. It consists of two resistors R_1 and R_2 which form a voltage divider. The hysteresis window is connected through the resistor R_2 to the output v_{out} and therefore changes instantaneous with the output. The window is centred around the voltage on terminal A which is where R_1 is connected to. From this information the following can be found:

$$v_{hys}(t) = \begin{cases} v_{thh} & \forall v_{out}(t) = v_H \\ v_{thl} & \forall v_{out}(t) = v_L \end{cases} \quad (2)$$

$$v_{thh} = k_1 \cdot (v_H - A) + A \quad (3)$$

$$v_{thl} = k_1 \cdot (v_L - A) + A \quad (4)$$

v_{thh} and v_{thl} is the upper and lower threshold voltage for the hysteresis window and k_1 is the scaling factor given by the resistor network R_1 and R_2 from fig. 3. From v_{thh} and v_{thl} it is possible to calculate the size of the hysteresis window:

$$v_{hw} = v_{thh} - v_{thl} = k_1 \cdot (v_H - v_L) \quad (5)$$

By isolating k_1 in eq. 5 and inserting it in eq. 3 and 4 the threshold voltages can be rewritten to:

$$v_{thh} = v_{hw} \frac{v_H - A}{v_H - v_L} + A \quad (6)$$

$$v_{thl} = v_{hw} \frac{v_L - A}{v_H - v_L} + A \quad (7)$$

These expressions are independable of the component values which is highly desired since it makes it easier to achieve desired design values.

When finding the expression for the carrier waveform v_C, the same method, as for the hysteresis window can largely be used. For the modulators to function properly the carrier voltage must be able to charge and discharge to the value of the hysteresis window as long as the audio input signal stays within the desired voltage span. To ensure that, the lowest voltage, the carrier voltage can have when the output is high, and the highest voltage, it can have when the output is low, is found. These limits are controlled by v_{out} and the signal on port B. The limits can be described as:

$$v_{Ch}(t) = k_2 \cdot (v_H - B) + B \quad (8)$$

$$v_{Cl}(t) = k_2 \cdot (v_L - B) + B \quad (9)$$

Where k_2 is the voltage divider consisting of the resistor network R_3 and R_4 from fig. 3 and v_{Ch} and v_{Cl} is the upper and lower limit the RC network is able to charge and discharge to. From this, the size of the window can be found:

$$v_{Cwin} = v_{Ch} - v_{Cl} = k_2 \cdot (v_H - v_L) \tag{10}$$

To find the limits for a specific input signal size, the following two equations are used to describe the limits of the input signal. Here it is assumed that the input signal is offset by the reference voltage, v_{ref}.

$$v_{inh} = v_{ref} + \frac{v_{span}}{2} \tag{11}$$

$$v_{inl} = v_{ref} - \frac{v_{span}}{2} \tag{12}$$

Where v_{inh} and v_{inl} is the highest and lowest expected input voltage. v_{ref} is the reference voltage which is applied on terminal A for the AIM and on terminal B for the HOM. v_{span} is the expected span of the input signal, i.e. the voltage difference between v_{inh} and v_{inl}. To simplify further calculations, the following is assumed:

$$v_{ref} = \text{mean}(v_H, v_L) \tag{13}$$

For the AIM, the audio input signal is send into terminal B. This means that it is possible to rewrite eq. 8 and 9 by substituting B with eq. 11 for eq. 9 and with eq. 12 for eq. 8. By isolating these for k_2 and inserting the expression for k_2 in eq. 8 and 9 again, an expression for the upper and lower limit of the carrier waveform is found. These equations have the input signal on terminal B as a variable.

$$v_{Ch_{AIM}}(t) = B + \frac{v_{span}(v_H - B) + v_{hw}(v_H - B)}{v_H - v_L + v_{span}} \tag{14}$$

$$v_{Cl_{AIM}}(t) = B + \frac{v_{span}(v_L - B) + v_{hw}(v_L - B)}{v_H - v_L + v_{span}} \tag{15}$$

For the HOM, the audio input signal is send into terminal A. This means that the size of the hysteresis window when it is offset must not exceed v_{Cwin} since it will result in clipping at smaller input signals than intended. To prevent this, the following is stated:

$$v_{Cwin} = v_{hw} \tag{16}$$

Since the audio input is on terminal A, A is substituted with eq. 11 and 12 in eq. 6 and 7 respectively. From this eq. 5, 10 and 16 is used to get:

$$v_{thh} - v_{thl} = k_2 \cdot (v_H - v_L) \tag{17}$$

By isolating k_2 and inserting it in eq. 8 and 9 the following expressions are found:

$$v_{Ch_{HOM}} = \frac{v_H + v_L + v_{hw} + v_{span}}{2} - \frac{v_{hw} v_{span}}{2(v_H - v_L)} \tag{18}$$

$$v_{Cl_{HOM}} = \frac{v_H + v_L - v_{hw} - v_{span}}{2} + \frac{v_{hw} v_{span}}{2(v_H - v_L)} \tag{19}$$

Now all the necessary equations to find the duty cycle for any given input signal both for the HOM and AIM modulator have been derived.

Since both modulators are first order modulators, they can be described using the equation for a RC network. By isolating the time in the equation for a first order RC network, the timings can be found to be:

$$t_{high} = \tau \cdot ln\left(\frac{v_{Ch} - v_{thl}}{v_{Ch} - v_{thh}}\right) \tag{20}$$

$$t_{low} = -\tau \cdot ln\left(\frac{v_{Cl} - v_{thl}}{v_{Cl} - v_{thh}}\right) \tag{21}$$

These timing equations hold true for both modulators. From the equations, it is now possible to calculate the frequency and duty cycle of each modulator's output.

$$f = \frac{1}{t_{high} + t_{low}} \tag{22}$$

$$D = \frac{t_{high}}{t_{high} + t_{low}} \tag{23}$$

4 Theoretical Results

The total harmonic distortion is strongly connected with how linear the relationship, between the input voltage and the duty cycle is. The relationship between the input voltage and the duty cycle can be found by sending a DC voltage into the modulator where after the duty cycle on the output is read. It is possible to do this because the switch frequency is significantly higher than the highest frequency of the audio signal. Therefore, the audio signal can be considered a DC signal when used by the modulator. For the following theoretical results, the values in table 1 have been used:

Table 1: Specifications

v_H	v_L	v_{hw}	v_{span}
1 V	0 V	0.5 V	1 V

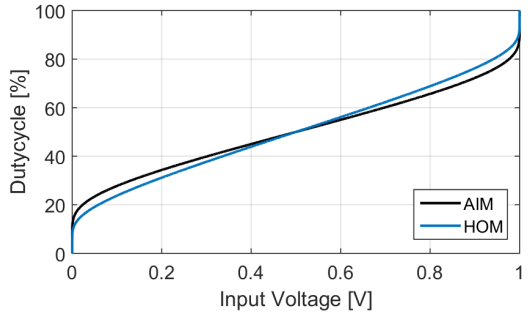

Fig. 7: Theoretical relation between the input voltage and the duty cycle of the output for the AIM and HOM

Figure 7 shows the DC transfer function of both modulators. It seems that the HOM assembles a straight line more and for a longer duration than the AIM. This would mean that the HOM in general is more transparent in the modulation than the AIM and would, due to that, have a lower total harmonic distortion (THD) than the AIM. To get a more precise view, a linear regression is found for the transfer function of each modulator and the correlation coefficient is calculated from that.

$$r^2_{AIM} = 0.9912 \tag{24}$$

$$r^2_{HOM} = 0.9954 \tag{25}$$

This is a clear indication that the transfer function of the HOM assembles a straight line more than the AIM.To further verify these results, a calculation of the theoretical THD of both modulators is performed. Figure 8 shows the theoretical THD found by using a sinusoid at 6.66 kHz with increasing amplitude as input.

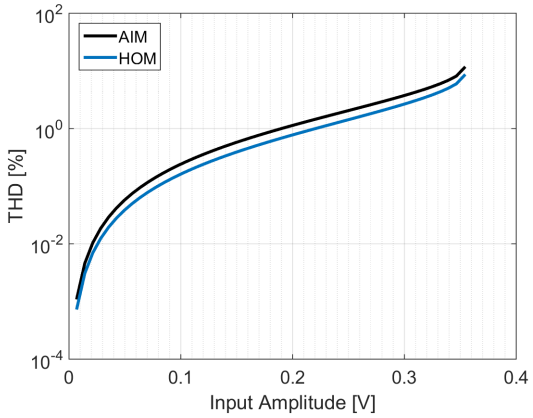

Fig. 8: Theoretical THD of both modulators

The THD calculations support the theory further as it clearly shows that a reduction in THD for the HOM, compared to the AIM, is to be expected.

The switch frequency of the output will change with the input voltage.

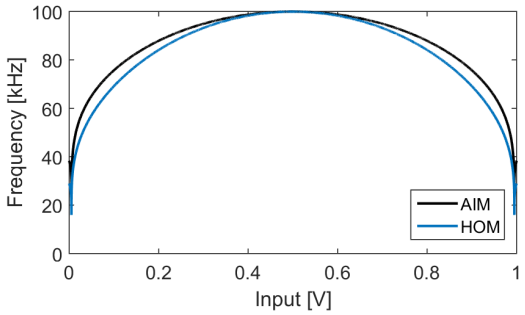

Fig. 9: Theoretical switch frequency of the output of each modulator

Figure 9 shows that the HOM tends to fall in switch frequency a bit faster than the AIM which is an unwanted behaviour. This is due to the fact that the modulator potentially will reach a switch frequency which is too low, for the modulator to operate properly, faster.

5 Measurements

5.1 Measurement Setup

To test the theory in practice, six test boards were made. This was done to ensure a consistency in the theory over multiple configurations. The boards were made in pairs such that one AIM board and one HOM board had the same specifications. All the boards were supplied with 5 V and had a reference voltage of 2.5 V. The comparator on the boards were able to deliver an output voltage from about 0.1 V to 4.85 V. The board specific specifications were the following:

Table 2: Board Specifications

Boards	1 and 2	3 and 4	5 and 6
f_{sw}	300 kHz	600 kHz	500 kHz
v_{hw}	1 V	1.6 V	0.6 V
v_{span}	4.95 V	2.1 V	1.2 V

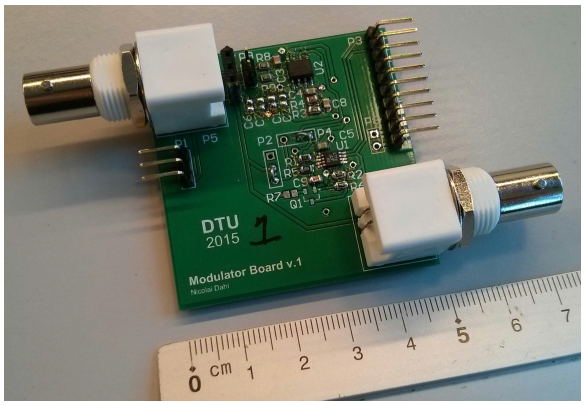

Fig. 10: Picture of test board 1. All the other boards looks similar.

5.2 Measurement results

For each board, three measurements were made; a measurement of the DC transfer function, a measurement of the switching frequency and a measurement of the THD. The measurement of the DC transfer function and the switching frequency was made by reading the duty cycle and frequency of the output when different input voltages were applied. The results of the DC transfer function can be seen on fig. 11a and the results of the switch frequency on fig. 11b. Both results are being compared with what was expected by the theory.

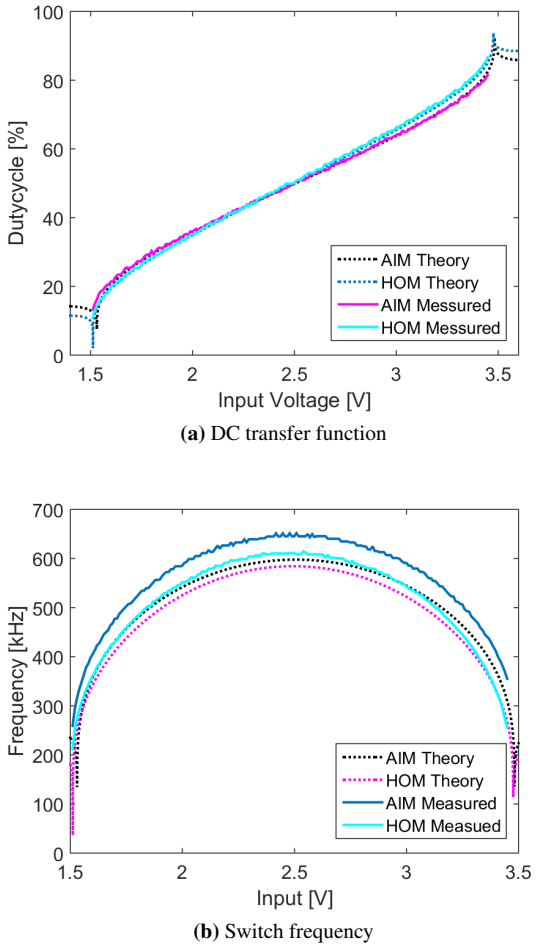

(a) DC transfer function

(b) Switch frequency

Fig. 11: Output of board 3 and 4 compared to the expected results

Figure 11a shows the DC transfer function for board 3 and 4 compared to the expected results. It is seen that the measured results and the theoretical results are close to identical. Similar results was obtained with the other boards. This supports the theory and indicates that the measurements of the THD should be close to the theory as well. Regarding the response of the switch frequency on fig. 11b it is possible to see that the measured switch frequency follows the same curve as the theory, however, the measured results are at a higher frequency than expected. This is due to stray capacitance and component tolerances since a small

adjustment in the capacitance in the theory results in a very accurate fit (fig. 12).

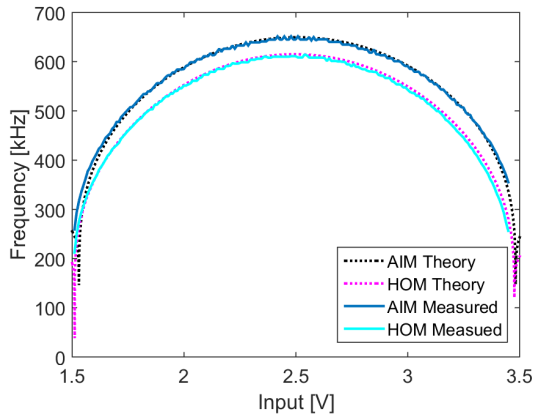

Fig. 12: Switch frequency with adjusted capacitance

The THD measurements were made with an active 2. order lowpass filter on the output of the modulator. The filter had a THD of around 0.5 % across the entire amplitude range which was used for testing.

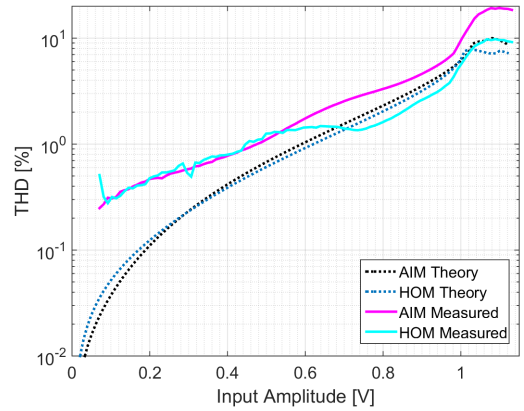

Fig. 13: Measured THD compared to the expected results

Figure 13 shows the measured THD compared to what was expected from the theory. It is seen that the measured results generally have a higher THD than expected yet still clearly follow the trends of the theory as the HOM has a lower THD than the AIM. The higher THD is partially due to the active filter but also due to noise in the circuitry. Especially at lower amplitudes it is possible to see the noise from the modulators from the jitter in the readings. Here it is seen that the HOM modulator seems to have noise problems up to a higher amplitude than the AIM, but this is for further studies. At the amplitude 0.7 V the measured THD of the HOM begins to move below the theoretical possible THD. This is probably due to tolerances in the resistors making the circuit behave a little different from the desired specifications.

6 Conclusion

This paper has presented the fundamental principles of PWM modulation. A thorough analysis of two simple self-oscillating modulators has been presented. That is the AIM modulator and the proposed HOM modulator. The analysis showed that the proposed HOM modulator can provide a more linear modulation than the AIM. This was evident from the modelling of the DC-DC transfer functions and the evaluated THD. Finally experimental results showed very good correlation with the presented theory and it was found that the proposed HOM modulator performs a 5th of a decade better in terms of THD. However the HOM modulator seems to be more susceptible to noise than the AIM. Future work will have to investigate this further.

References

[1] K. Nielsen, "Audio Power Amplifier Techniques With Energy Efficient Power Conversion", Ph.D. thesis, Volume 1, Technical University of Denmark, 1998.

[2] M. Duraj, N. E. Iversen, L. P. Petersen and P. Boström, "Self-oscillating 150 W switch-mode amplifier equipped with eGaN-FETs", in AES Convention 139th, New York, October 29-November 1, 2015.

[3] B. Putzeys, "Simple Self-Oscillating Class D Amplifier with Full Output Filter Control", in AES Convention 118th, Barcelona, May 28-31, 2005.

[4] S. Poulsen and M. A. E. Andersen , "Simple PWM modulator topology with excellent dynamic behaviour", in Applied Power Electronics Conference and Exposition, 2004.

[5] D. Nielsen, A. Knott, G. Pfaffinger and M. A.E. Andersen, "Investigation of switching frequency variations and EMI properties in self-oscillating class D amplifiers", in AES Convention 127th, New York, October 2009

[6] E. Gaalaas, "Class D Audio Amplifiers: What, Why, and How", Analog Devices, June 2006

[7] S. Poulsen, "Global Loop Integrating Modulator", World Intellectual Property Organization, November 2004.

[8] B. Putzeys ,"Power Amplifier", U.S. Patent No.: US 7,113,038 B2, September 2006.

[9] L. Risbo, M. C. W. Hœyerby and M. A. E. Andersen , "A Versatile Discrete-Time Approach for Modeling Switch-Mode Controllers", IEEE PESC, 2008.

[10] M. C. W. Hœyerby, "High-Performance Control in Radio Frequency Power Amplification Systems", Ph.D. Thesis, Technical University of Denmark, 2008.

[11] S. Poulsen and M. A.E. Andersen, "Self-Oscillating PWM Modulators, A Topological Comparison", in IPMHVC 26th, 2004

[12] S. Poulsen, "Towards Active Transducers", Ph.D. thesis, Technical University of Denmark, 2004

[13] A. Knott, G. Pfaffinger and M. A. E. Andersen , "A Self-Oscillating Control Scheme for a Boost Converter Providing a Controlled Output Current", IEEE transactions on Power Electronics, January 2009.